

---

# Comparison of Maximum Likelihood and GAN-based training of Real NVPs

---

Ivo Danihelka<sup>1,2</sup> Balaji Lakshminarayanan<sup>1</sup> Benigno Uria<sup>1</sup> Daan Wierstra<sup>1</sup> Peter Dayan<sup>3</sup>

## Abstract

We train a generator by maximum likelihood and we also train the same generator architecture by Wasserstein GAN. We then compare the generated samples, exact log-probability densities and approximate Wasserstein distances. We show that an independent critic trained to approximate Wasserstein distance between the validation set and the generator distribution helps detect overfitting. Finally, we use ideas from the one-shot learning literature to develop a novel fast learning critic.

## 1. Introduction

There has been a substantial recent interest in deep generative models. Broadly speaking, generative models can be classified into *explicit* models where we have access to the model likelihood function, and *implicit* models which provide a sampling mechanism for generating data, but do not need to explicitly define a likelihood function. Examples of explicit models are variational auto-encoders (VAEs) (Kingma & Welling, 2013; Rezende et al., 2014) and PixelCNN (Oord et al., 2016). Examples of implicit generative models are generative adversarial networks (GANs) (Goodfellow et al., 2014) and stochastic simulator models. Explicit models are typically trained by maximizing the likelihood or its lower bound; they are popular in probabilistic modeling as the training procedure optimizes a well-defined quantity and the likelihood can be used for model comparison and selection. However likelihood is not about human perception (Theis et al., 2015).

Recently, GAN-based training has emerged as a promising approach for learning implicit generative models. In particular, generators trained using GAN-based approaches have shown to be capable of generating photo-realistic samples. There is a lot of interest in understanding the the properties of the learned generators in GANs and comparing them with traditional likelihood-based methods. One step

<sup>1</sup>Google DeepMind, London, United Kingdom <sup>2</sup>CoMPLEX, Computer Science, UCL <sup>3</sup>Gatsby Unit, UCL. Correspondence to: Ivo Danihelka <danihelka@google.com>.

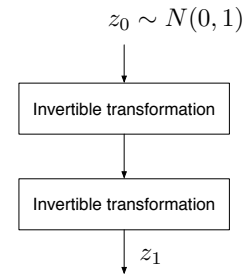


Figure 1. The generator is a real NVP with multiple invertible transformations.

in this direction was the quantitative analysis by Wu et al. (2016) who evaluate the (approximate) likelihood of decoder based models using annealed importance sampling (AIS). We use a different approach to provide additional insights. We use a tractable generator architecture for which the log-probability densities can be computed exactly. We train the generator architecture by maximum likelihood and we also train the *same* generator architecture by GAN. We then compare the properties of the learned generators.

Concretely, we use real non-volume preserving transformation (real NVP) (Dinh et al., 2016) as the generator. We compare training by maximum likelihood to training by Wasserstein GAN (WGAN) (Arjovsky et al., 2017). In WGAN, a critic learns to approximate the Wasserstein distance between the data and the generator distribution. The generator learns to minimize the critic’s approximation of the Wasserstein distance. WGAN has a well defined training procedure and allowed us to train a non-traditional GAN generator. Another advantage of WGAN is that the critic’s approximation of the Wasserstein distance can be used to detect overfitting as well as to compare different models. We discuss this more in Section 3.5.

WGAN worked for us better than other GAN methods (Jensen-Shannon divergence or  $-\log D(x)$ ). We intend to communicate the found interesting differences from training by maximum likelihood. After describing the generator and the critic in Section 2, we report some perhaps surprising findings in Section 3:

1. Generators trained by WGAN produce more globally coherent samples even from a relatively shallow gen-

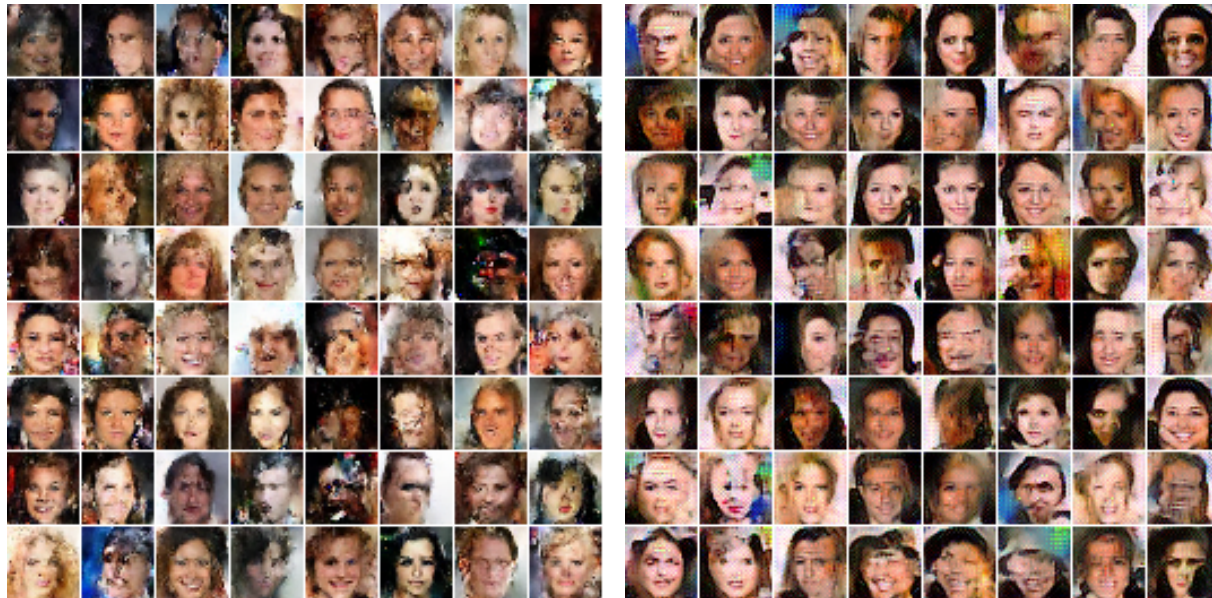


Figure 2. **Left:** Samples from a generator NVP3 trained by maximum likelihood. **Right:** Samples from a generator NVP3 trained by WGAN. Both generators had the same architecture. The WGAN samples would look better if using the improved training of WGAN-GP (Gulrajani et al., 2017). The other conclusions are similar for WGAN-GP.

erator.

2. Minimization of the approximate Wasserstein distance does not correspond to minimization of the negative log-probability density. The negative log-probability densities became worse than densities from a uniform distribution.

We also report a few findings about the approximate Wasserstein distance:

1. An approximation of the Wasserstein distance ranked correctly generators trained by maximum likelihood.
2. The approximate Wasserstein distance between the training data and the generator distribution became smaller than the distance between the test data and the generator distribution. This overfitting was observed for generators trained by maximum likelihood and also for generators trained by WGAN.

Finally, we use the ability to compare different models when evaluating a novel fast learning critic in Section 4.

## 2. Setup

### 2.1. Generator

In all our experiments, the generator is a real-valued non-volume preserving transformation (NVP) (Dinh et al.,

2016). The generator is schematically represented in Figure 1. The generator starts with *latent* noise  $z_0$  from the standard normal distribution. The noise is transformed by a sequence of invertible transformations to a generated image  $z_1$ . Like other generators used in GANs, the generator does not add independent noise to the generated image.

Unlike other GAN generators, we are able to compute the log-probability density of the generated image  $z_1$  by:

$$\log p_{Z_1}(z_1) = \log p_{Z_0}(z_0) - \log \left| \det \frac{\partial z_1}{\partial z_0} \right| \quad (1)$$

where  $\log p_{Z_0}(z_0)$  is the log-probability density of the standard normal distribution. The determinant of the  $\frac{\partial z_1}{\partial z_0}$  Jacobian matrix can be computed efficiently, if each transformation has a triangular Jacobian (Dinh et al., 2016).

We can also compute the log-probability density assigned to an image by running the inverse of the transformations. The inferred  $z_0$  can be then plugged to Equation 1.

We use a generator with the convolutional multi-scale architecture designed by Dinh et al. (2016). Concretely, we use 3 different generator architectures with 1, 2 and 3 multi-scale levels. In figures, these generators are labeled NVP1, NVP2, NVP3 and have 7, 13 and 19 non-volume preserving transformations. Each transformation uses 4 residual blocks. In total, the generator NVP3 has  $19 \times 4 = 76$  layers. It is a very deep generator. To have the same training and testing conditions, we use no batch normalization in the generator.



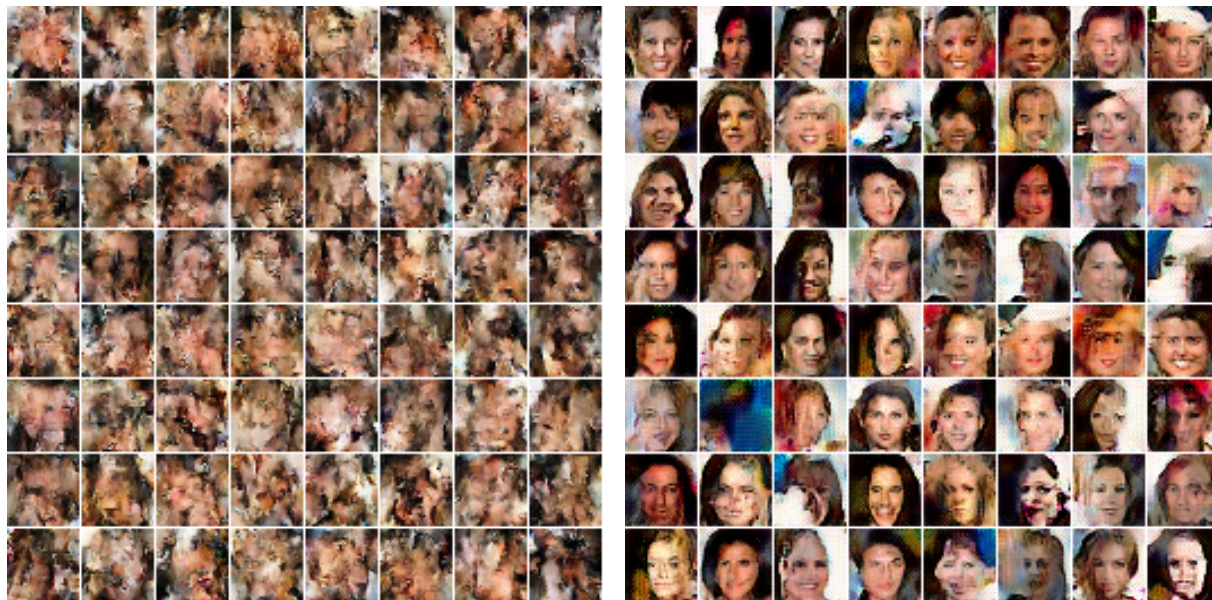


Figure 3. **Left:** Samples from the shallow generator NVP1 trained by maximum likelihood. **Right:** Samples from the same shallow architecture trained by WGAN.

## 2.2. Critic

Wasserstein GAN (WGAN) (Arjovsky et al., 2017) uses a critic instead of a discriminator. The critic is trained to provide an approximation of the Wasserstein distance between the real data distribution  $P_r$  and the generator distribution  $P_g$ . The approximation is based on the Kantorovich-Rubinstein duality:

$$W(P_r, P_g) \propto \max_f \mathbb{E}_{x \sim P_r} [f(x)] - \mathbb{E}_{x \sim P_g} [f(x)] \quad (2)$$

where  $f : \mathbb{R}^D \rightarrow \mathbb{R}$  is a Lipschitz continuous function. In practice, the critic  $f$  is a neural network with clipped weights to have bounded derivatives. The critic is trained to produce high values at real samples and low values at generated samples. The difference of the expected critic values then approximates the Wasserstein distance. The approximation is scaled by the Lipschitz constant for the critic (Arjovsky et al., 2017). After training the critic for the current generator distribution, the generator can be trained to minimize the approximate Wasserstein distance.

We follow closely the original WGAN implementation<sup>1</sup> and use a DCGAN (Radford et al., 2015) based critic. The implementation uses learning rate 0.00005, batch size 64 and clips the critic weights to a fixed box  $[-0.01, 0.01]$ . The critic is updated 100 times in the first 25 generator steps and also after every 500 generator steps, otherwise the critic is updated 5 times per generator step.

<sup>1</sup><https://github.com/martinarjovsky/WassersteinGAN>

We rescale the images to  $[-1, 1]$  range before feeding them to the critic.

## 2.3. Datasets

We train on  $28 \times 28$  images from MNIST (LeCun et al., 1998) and on  $32 \times 32$  images from the CelebFaces Attributes Dataset (CelebA) (Liu et al., 2015). The CelebA dataset contains over 200,000 celebrity images. During training we augment the CelebA dataset to also include horizontal flips of the training examples as done by Dinh et al. (2016).

## 2.4. Data Preprocessing

We convert the discrete pixel intensities from  $\{0, \dots, 255\}^D$  to continuous noisy images from  $[0, 256]^D$  by adding a uniform noise  $u \in [0, 1]^D$  to each pixel intensity. The computed log-probability density will be then a lower bound for the log-probability mass (Theis et al., 2015):

$$\int_{[0,1]^D} \log p(x+u) du \leq \log \int_{[0,1]^D} p(x+u) du \quad (3)$$

Finally, before feeding the pixel intensities to a network, we divide the pixel intensities by 256. This is a simple non-volume preserving transformation. If the noisy image is  $z_2 = x+u$  and the image with scaled intensities is  $z_1 = \frac{z_2}{256}$

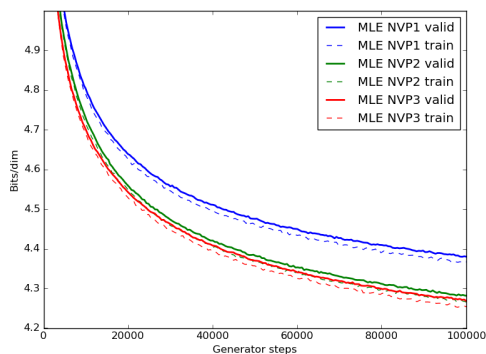


Figure 4. The negative log-probability density of real NVPs in  $bits/dim$  on CelebA  $32 \times 32$  images. The generators were trained by maximum likelihood estimation (MLE). The loss is slightly higher on the validation set.

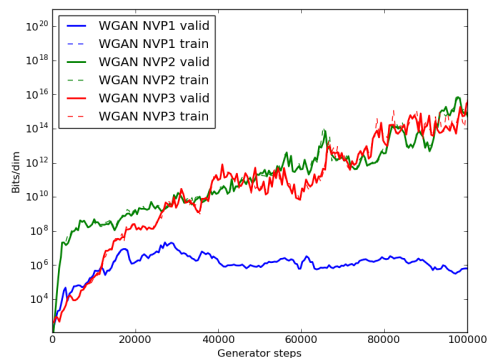


Figure 5. The negative log-probability density of real NVPs trained by WGAN on CelebA. Note the logarithmic scale on y-axis.

then the log-probability density of the noisy image is:

$$\log p_{Z_2}(z_2) = \log p_{Z_1}(z_1) - \log \left| \det \frac{\partial z_2}{\partial z_1} \right| \quad (4)$$

$$= \log p_{Z_1}(z_1) - D \log 256 \quad (5)$$

where  $D$  is the number of dimensions in the image (e.g.,  $D = 32 \times 32 \times 3$ ). For example, if an uninformed model assigns uniform probability density  $p_{Z_1}(z_1) = 1$  to all  $z_1 \in [0, 1]^D$ , the model would require  $\log_2(256) = 8$  bits/dim to describe an image. The reported negative log-probability density then corresponds to an upper bound on compression loss in bits/dim.

### 3. Results

We trained the same generator architecture by maximum likelihood and by WGAN. We will now compare the effect of these two different objectives.

#### 3.1. Generated Samples

Figure 2 shows samples from a generator trained by maximum likelihood and from another generator trained by WGAN. Both generators have the same number of parameters and the same architecture.

The generator trained by WGAN seems to produce more coherent faces. The effect is more apparent when looking at samples produced from a shallower generator in Figure 3. The shallow generator NVP1 learned to produce only locally coherent image patches if trained by maximum likelihood.

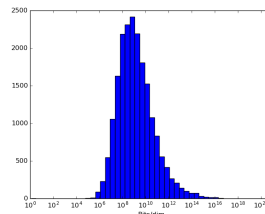


Figure 6. The histogram of negative log-probability densities on the CelebA validation set. The generator NVP3 was trained by WGAN.

#### 3.2. Log-probability Density

Figure 4 shows the negative log-probability density for generators trained by maximum likelihood estimation (MLE). The shallowest generator NVP1 obtained the worse performance there. The generators show only a small amount of overfitting to the training set. The validation loss is slightly higher than the training loss.

Generators trained by WGAN have their negative log-probability densities shown in Figure 5. The figure has a completely different y-axis. The negative log-probability densities get worse when training by WGAN. The training and validation losses overlap.

A generator can get infinite negative log-probability if it assigns zero probability to an example. To check this possibility, we analysed the negative log-probabilities assigned to all validation examples. Figure 6 shows the histogram of negative log-probabilities. We see that all 19867 validation examples have low log-probabilities. A similar histogram was obtained also for the training set. So the bad average log-probability is not caused by a single outlier.

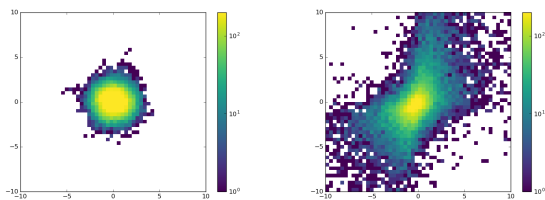


Figure 7. **Left:** 2D histogram of 2 latent variables for examples from the CelebA validation set. The generator was NVP3 trained by maximum likelihood. **Right:** 2D histogram of 2 latent variables for generator NVP3 trained by WGAN.

We further inspected the negative log-probability density of generated samples. We observed that the average negative log-probability density of generated samples is **-1.12** bits/dim. The negative sign is not a typo. The negative log-probability density can be negative, if the probability density is bigger than 1. In contrast, the NVP3 generator trained by maximum likelihood assigned on average 4.27 bits/dim to the validation examples and 4.35 bits/dim to its own generated samples.

The problematic negative log-probability densities from WGAN were not limited to the CelebA dataset. Generators trained by WGAN had high negative log-probability densities also on MNIST (Figure 13). A deep generator trained by WGAN learns a distribution lying on a low dimensional manifold (Figure 17 in the appendix). The generator is then putting the probability mass only to a space with a near-zero volume. We may need a more powerful critic to recognize the excessively correlated pixels. Approximating the likelihood by annealed importance sampling (Wu et al., 2016) would not discover this problem, as their analysis assumes a Gaussian observation model with a fixed variance.

The problem is not unique to WGAN. We also obtained near-infinite negative log-probability densities when training GAN to minimize the Jensen-Shannon divergence (Goodfellow et al., 2014).

### 3.3. Distribution of Latent Variables

One of the advantages of real NVPs is that we can infer the original latent  $z_0$  for a given generated sample. We know that the distribution of the latent variables is the prior  $N(0, 1)$ , if the given images are from the generator. We are curious to see the distribution of the latent variables, if the given images are from the validation set.

In Figure 7, we display a 2D histogram of the first 2 latent variables  $z_0[1], z_0[2]$ . The histogram was obtained by inferring the latent variables for all examples from the validation set. When the generator was trained by maxi-

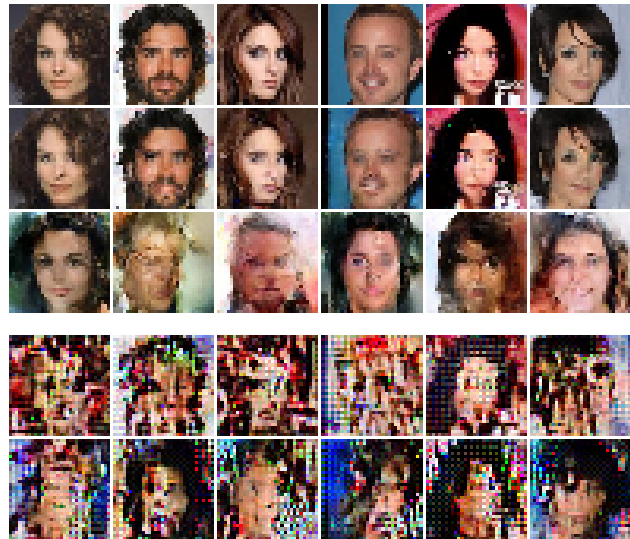


Figure 8. **From top to bottom:** 1) Original images from the CelebA validation set. 2) Reconstructions from the first half of latent variables. The generator was NVP3 trained by MLE. 3) Reconstructions from the second half of latent variables for MLE. 4) Reconstructions from the first half of latent variables if the generator was trained by WGAN. 5) Reconstructions from the second half of latent variables for WGAN.

imum likelihood, the inferred latent variables had the following means and standard deviations:  $\mu_1 = 0.05, \mu_2 = 0.05, \sigma_1 = 1.06, \sigma_2 = 1.03$ . In contrast, the generator trained by WGAN had inferred latent variables with significantly larger standard deviations:  $\mu_1 = 0.02, \mu_2 = 1.62, \sigma_1 = 3.95, \sigma_2 = 8.96$ .

When generating the latent variables from the  $N(0, 1)$  prior, the samples from the generator trained by WGAN would have a different distribution than the validation set.

### 3.4. Partial Reconstructions

Real NVPs are invertible transformations and have perfect reconstructions. We can still visualize reconstructions from a partially resampled latent vector. Gregor et al. (2016) and Dinh et al. (2016) visualized ‘conceptual compression’ by inferring the latent variables and then resampling a part of the latent variables from the normal  $N(0, 1)$  prior. The subsequent reconstruction should still form a valid image. If the original image was generated by the generator, the partially resampled latent vector would still have the normal  $N(0, 1)$  distribution.

Figure 8 shows the reconstructions if resampling the first half or the second half of the latent vector. The generator trained by maximum likelihood (MLE) has partial reconstructions similar to generated samples. In comparison,

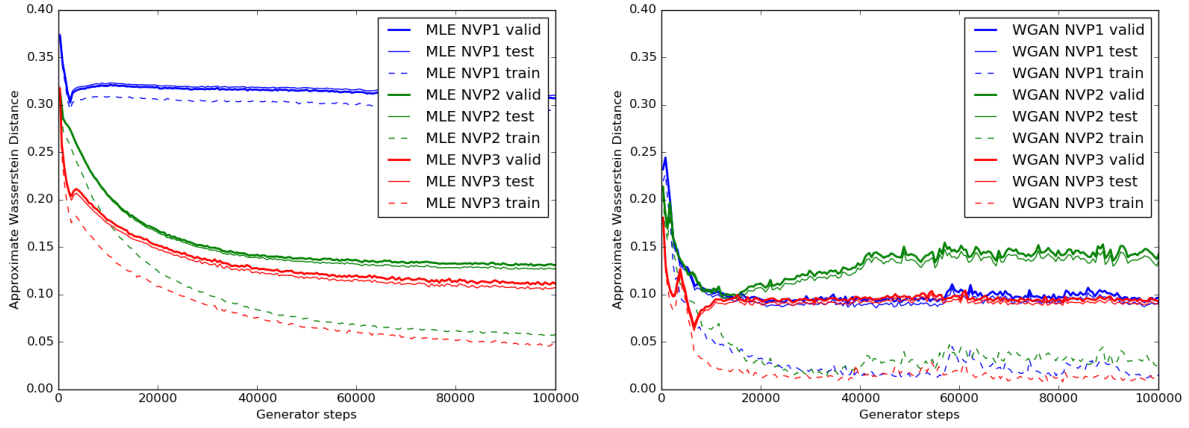


Figure 9. **Left:** The approximate Wasserstein distance for real NVPs trained by maximum likelihood on CelebA. **Right:** The approximate Wasserstein distance for real NVPs trained by WGAN. The Wasserstein distance was approximated by an independent critic.

the partial reconstructions from the generator trained by WGAN do not resemble samples from WGAN. This again indicates that the validation examples have a different distribution than WGAN samples.

### 3.5. Wasserstein Distance

We will now look at the approximate Wasserstein distance between the validation data and the generator distribution. To approximate the Wasserstein distance, we will use the duality in Equation 2. We will train another critic to assign high values to validation samples and low values to generated samples. This *independent* critic will be used only for evaluation. The generator will not see the gradients from the independent critic.

The independent critic is trained to maximize:

$$\hat{W}(x_{valid}, x_g) = \frac{1}{N} \sum_{i=1}^N \hat{f}(x_{valid}[i]) - \frac{1}{N} \sum_{i=1}^N \hat{f}(x_g[i]) \quad (6)$$

where  $x_{valid}$  is a batch of samples from the validation set,  $x_g$  is a batch of generated samples and  $\hat{f}$  is the independent critic.

We will keep the Lipschitz constant of the independent critic approximately constant by always using same architecture and the same weight clipping for the independent critic. We can then compare the approximate Wasserstein distances from different experiments.

Figure 9-left shows the approximate Wasserstein distance between the validation set and the generator distribution. The first thing to notice is the correct ordering of generators trained by maximum likelihood. The deepest generator NVP3 has the smallest approximate distance from the validation set, as indicated by the thick solid lines.

We also display an approximate distance between the training set and generator distribution:

$$\hat{W}(x_{train}, x_g) \quad (7)$$

and the approximate distance between the test set and the generator distribution:

$$\hat{W}(x_{test}, x_g) \quad (8)$$

where  $x_{train}$  is a batch of training examples,  $x_{test}$  is a batch of test examples and  $\hat{W}$  is the approximate Wasserstein distance computed by Equation 6. We are misusing the independent critic here. We are asking the independent critic to assign values to training and test examples. The independent critic was trained only to assign values to validation examples and to generated samples. This leads to a desirable effect: We can detect whether the generator overfits the training data. If the training examples have the same distribution as the test examples, we should observe:

$$\mathbb{E} [\hat{W}(x_{train}, x_g)] = \mathbb{E} [\hat{W}(x_{test}, x_g)] \quad (9)$$

In practice, the empirical distribution of the training data is not the same as the distribution of the test data. The generated samples  $x_g$  can be more similar to the training data than to the test data.

Figure 9 clearly shows that:

$$\hat{W}(x_{train}, x_g) < \hat{W}(x_{test}, x_g) \quad (10)$$

for the trained generators. The approximate distance between the test set and the generator distribution is a little bit smaller than the approximate distance between the validation set and the generator distribution. The approximate distance between the training set and the generator distribution is much smaller. The generators are overfitting the training set.





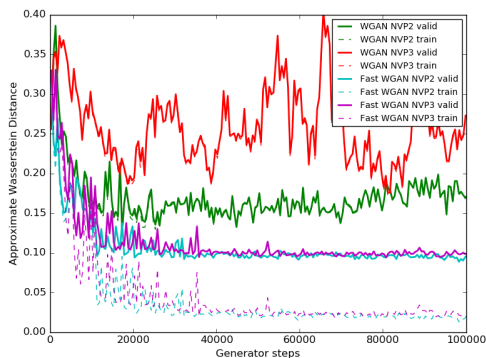


Figure 12. The approximate Wasserstein distance on CelebA when updating the critic less often. The shown Wasserstein distance was approximated by an independent critic.

gated activations (Figure 10) on the residual connections (Oord et al., 2016). The features from the batch of extra generator samples are averaged over the batch dimension to produce the distribution embedding.

Algorithm 1 shows the usage of the critic. The embedding remains the same when running the critic on real or generated samples. The critic would become the original WGAN critic, if using zeros instead of the distribution embedding. We use batch size 64 and we also use 64 extra generator samples.

The weights used to produce the embedding of the distribution do not need to be clipped and we do not clip them.

When training a generator, we do not use the gradients with respect to the extra generator samples. The generator is only trained with the gradient of the approximate Wasserstein distance with respect to  $x_g$ .

#### 4.2. Fast Learning Results

Figure 12 compares training without and with the fast learning critic. The critic was intentionally updated less frequently by gradient descent to demonstrate the benefits of the fast learning. The critic was updated 100 times in the first 25 generator steps and also after every 500 generator steps, otherwise the critic is updated only 2 times per generator step. The independent critic was still updated at least 5 times per generator step to keep all measurements comparable.

Without the fast learning critic, the generator failed to produce samples similar to the data examples. The fast learning critic may be important for conditional models and for video modeling. We do not have multiple real samples for a situation there.

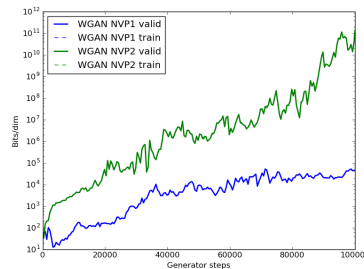


Figure 13. The negative log-probability density of real NVPs trained by WGAN on MNIST. The validation loss and the training loss overlap.

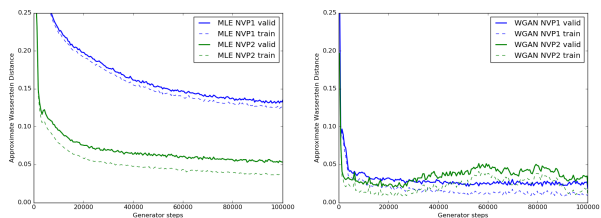


Figure 14. **Left:** The approximate Wasserstein distance for real NVPs trained by maximum likelihood with MNIST. **Right:** The approximate Wasserstein distance for real NVPs trained by WGAN. The Wasserstein distance was approximated by an independent critic.

## 5. Discussion

In our experiments, we used two tools for the evaluation of generators. First, we used a real NVP to compute the exact log-probability densities. Second, we used an independent critic to compare the approximate Wasserstein distances on the validation set. The independent critic is very generic. The critic only needs samples from two distributions.

The approximate Wasserstein distance from the independent critic allows us to compare different generator and critic architectures. If we care about Wasserstein distances, we should be comparing generators based on the approximate Wasserstein distance to the validation set.

The log-probability densities are less useful for generator comparison when the generators are generating only a subset of the data. On the other hand, when doing lossless compression, we care about log-probabilities (Theis et al., 2015). When using real NVPs we can even jointly optimize both objectives (Figure 15 and Figure 16).

We show one additional usage of real NVPs for Adversarial Variational Bayes (Mescheder et al., 2017) evaluation in the appendix.



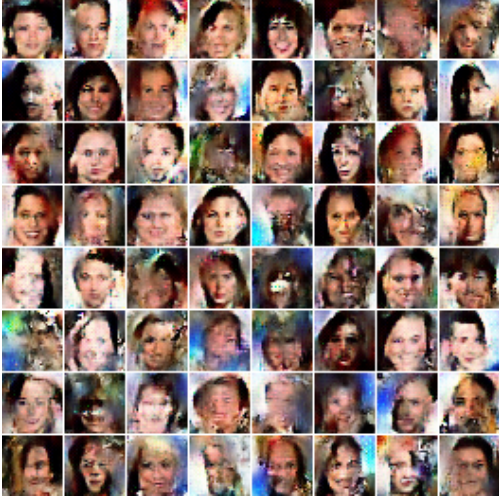


Figure 15. Samples generated from the shallow NVP1 trained by combined MLE+WGAN objectives. The samples are more globally coherent than samples from NVP1 trained by MLE alone (Figure 3-left).

## Acknowledgments

We want to thank Mihaela Rosca, David Warde-Farley, Shakir Mohamed, Edward Lockhart, Arun Nair and Chris Burgess for many inspiring discussions. We also thank the very helpful anonymous reviewer for suggesting to inspect the rank of the Jacobian matrix.

## A. Log-probability Density Ratio Evaluation

Real NVPs are not limited to the computation of negative log-probability densities of visible variables. For example, a real NVP can be used as an encoder in Adversarial Variational Bayes (Huszár, 2017; Mescheder et al., 2017). We were able to measure the gap between the unbiased  $KL$  estimate  $\log q(z|x) - \log p(z)$  and its approximation from GAN. Figure 18 shows that Adversarial Variational Bayes underestimates the  $KL$  divergence. The discriminator would need to output  $\text{logit}(D(x)) = -KL$  to represent the  $KL$ .

After measuring the problem, we can start thinking how to mitigate it. It would be possible to use auto-regressive discriminators (Oord et al., 2016) to decompose the large  $KL$  divergence to multiple smaller terms:

$$\log \frac{q(z|x)}{p(z)} = \sum_i \log q(z_i|x, z_{1:i-1}) - \log p(z_i) \quad (11)$$

where  $p(z_i)$  is the independent Gaussian prior.

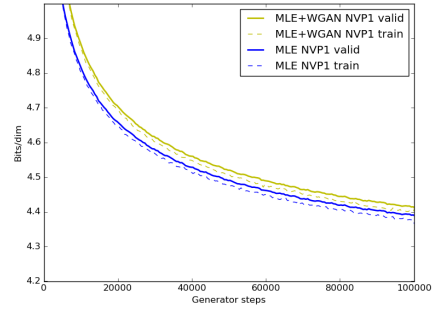


Figure 16. The negative log-probability density of NVP1 trained by combined MLE+WGAN objectives is not much worse than the negative log-probability of NVP1 trained by MLE alone.

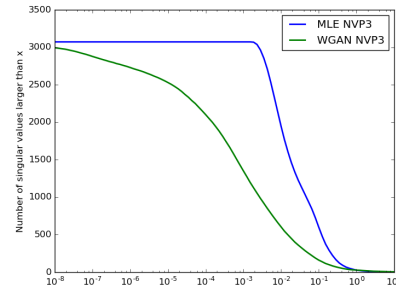


Figure 17. Inspection of the rank of the Jacobian matrix of the generator transformation for CelebA  $32 \times 32$ . The WGAN generator has a Jacobian with a low rank. The WGAN distribution then lies on a low dimensional manifold as predicted by Arjovsky & Bottou (2017).

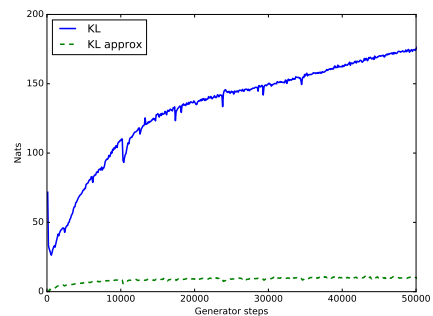


Figure 18. The unbiased  $KL(q(z|x)||p(z))$  value and the approximation of the  $KL$  from a discriminator. The discriminator was trained to recognize samples from the encoder from the samples from the prior. The discriminator is not representing well large  $KL$  divergences.

## References

- Arjovsky, M. and Bottou, L. Towards Principled Methods for Training Generative Adversarial Networks. *arXiv preprint arXiv:1701.04862*, 2017.
- Arjovsky, Martin, Chintala, Soumith, and Bottou, Léon. Wasserstein GAN. *arXiv preprint arXiv:1701.07875*, 2017.
- Dinh, Laurent, Sohl-Dickstein, Jascha, and Bengio, Samy. Density estimation using real NVP. *arXiv preprint arXiv:1605.08803*, 2016.
- Goodfellow, Ian, Pouget-Abadie, Jean, Mirza, Mehdi, Xu, Bing, Warde-Farley, David, Ozair, Sherjil, Courville, Aaron, and Bengio, Yoshua. Generative adversarial nets. In *Advances in neural information processing systems*, pp. 2672–2680, 2014.
- Gregor, Karol, Besse, Frederic, Rezende, Danilo Jimenez, Danihelka, Ivo, and Wierstra, Daan. Towards conceptual compression. In *Advances In Neural Information Processing Systems*, pp. 3549–3557, 2016.
- Gulrajani, Ishaan, Ahmed, Faruk, Arjovsky, Martin, Dumoulin, Vincent, and Courville, Aaron. Improved training of wasserstein gans. *arXiv preprint arXiv:1704.00028*, 2017.
- Huszár, Ferenc. Variational inference using implicit models, part I: Bayesian logistic regression. <http://www.inference.vc/variational-inference-with-implicit-probabilistic-models-part-1-2/>, 2017.
- Kingma, Diederik P and Welling, Max. Auto-encoding variational Bayes. *arXiv preprint arXiv:1312.6114*, 2013.
- LeCun, Yann, Bottou, Léon, Bengio, Yoshua, and Haffner, Patrick. Gradient-based learning applied to document recognition. *Proceedings of the IEEE*, 86(11):2278–2324, 1998.
- Liu, Ziwei, Luo, Ping, Wang, Xiaogang, and Tang, Xiaoou. Deep learning face attributes in the wild. In *Proceedings of International Conference on Computer Vision (ICCV)*, 2015.
- Mescheder, L., Nowozin, S., and Geiger, A. Adversarial Variational Bayes: Unifying Variational Autoencoders and Generative Adversarial Networks. *arXiv preprint arXiv:1701.04722*, 2017.
- Muandet, Krikamol, Fukumizu, Kenji, Sriperumbudur, Bharath, and Schölkopf, Bernhard. Kernel mean embedding of distributions: A review and beyonds. *arXiv preprint arXiv:1605.09522*, 2016.
- Oord, Aaron van den, Kalchbrenner, Nal, Vinyals, Oriol, Espeholt, Lasse, Graves, Alex, and Kavukcuoglu, Koray. Conditional image generation with PixelCNN decoders. *arXiv preprint arXiv:1606.05328*, 2016.
- Radford, Alec, Metz, Luke, and Chintala, Soumith. Un-supervised representation learning with deep convolutional generative adversarial networks. *arXiv preprint arXiv:1511.06434*, 2015.
- Rezende, Danilo Jimenez, Mohamed, Shakir, and Wierstra, Daan. Stochastic backpropagation and approximate inference in deep generative models. In *Proceedings of The 31st International Conference on Machine Learning*, pp. 1278–1286, 2014.
- Santoro, Adam, Bartunov, Sergey, Botvinick, Matthew, Wierstra, Daan, and Lillicrap, Timothy. One-shot learning with memory-augmented neural networks. *arXiv preprint arXiv:1605.06065*, 2016.
- Theis, Lucas, Oord, Aäron van den, and Bethge, Matthias. A note on the evaluation of generative models. *arXiv preprint arXiv:1511.01844*, 2015.
- Vinyals, Oriol, Blundell, Charles, Lillicrap, Tim, Wierstra, Daan, et al. Matching networks for one shot learning. In *Advances in Neural Information Processing Systems*, pp. 3630–3638, 2016.
- Wu, Yuhuai, Burda, Yuri, Salakhutdinov, Ruslan, and Grosse, Roger. On the quantitative analysis of decoder-based generative models. *arXiv preprint arXiv:1611.04273*, 2016.